Degeneration of the long biceps tendon of the shoulder: Comparison of MR imaging with gross anatomy and histology.

F. M. Buck[1], H. Grehn[2], M. Hilbe[3], S. Manzanell[4], and J. Hodler[1]

[1]Department of Radiology, Balgrist University Hospital, Zurich, Switzerland, [2]Orthopedic Surgery, Balgrist University Hospital, Zurich, Switzerland, [3]Institute of Veterinary Pathology, Vetsuisse Faculty, University of Zurich, Zurich, Switzerland, [4]MSRU, Equine Hospital, Vetsuisse Faculty, University of Zurich, Zurich, ZH, Switzerland

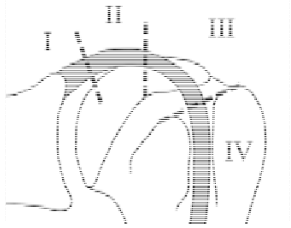

Figure 1: Subdivision of proximal long biceps tendon. Segment I: biceps anchor and its attachment. II: distal of segment 1 to most cranial point of the humeral head. III: curved course of the tendon around the humeral head. IV: distal from the entrance of the tendon into the intertubercular sulcus.

Background

Diagnosis of biceps tendinopathy in the shoulder is difficult due to its complex anatomy, artifacts, and degeneration.

Purpose

To relate alterations of biceps tendon diameter and signal to gross anatomical and histological findings.

Materials and Methods

Fifteen cadaveric shoulders underwent MR imaging using a 1.5T system. T1-weighted (T1w; section thickness, 3mm; repetition time [TR], 539 msec; echo time [TE], 15 msec; field of view, 14x14 cm; matrix size, 512x512; numbers of excitations [NEX], 2), T2-weighted fat-saturated (T2w fs) fast spin-echo (section thickness, 3 mm; TR, 3040 msec; TE, 71 msec; field of view, 14x14 cm; matrix, 512x512; NEX, 1; echo train length [ETL], 7), and proton density-weighted fat-saturated (PDw fs; section thickness, 3 mm; TR, 2640 msec; TE, 15 msec; field of view, 14x14 cm; matrix, 512x512; NEX, 2; ETL, 7) spin-echo sequences were acquired in the transverse, angled sagittal (parallel to the glenoid joint surface), and angled coronal (perpendicular to the glenoid joint surface) planes. Alterations of biceps tendon diameter and signal were graded (Grade 0: black as cortical bone. Grade 1: signal between cortical bone and deltoid muscle. Grade 3: isointense to deltoid muscle. Grade 3: between deltoid muscle and subcutaneous fat (T1w) / joint fluid (T2w fs, PDw fs). Grade 4: brighter than fat (T1w) / joint fluid (T2w fs, PDw fs) by two readers independently and blinded towards anatomical and histological findings. The positions of tendon abnormalities were measured with respect to the attachment of the tendon at the glenoid. In addition, the tendon was divided into four segments (Figure 1). MR findings were related to gross anatomical and histological assessments. Paraffin embedded, hematoxylin and eosin (HE) stained, 2 – 4 µm thick sections and methylmethacrylate embedded, toluidine blue stained thick slides were evaluated. In addition, alcian blue and Masson's trichrome stains were performed to detect an increase in mucopolysaccharid acids in areas of mucoid degeneration. Van Giesson stain was used to demonstrate connective tissue in areas of mucoid degeneration and to visualize fibrocartilaginous metaplasia. Mucoid degeneration (Figure 2), fatty infiltration, lipoid degeneration was diagnosed. On the HE slides the distance of pathologic changes from the bony attachment of the tendon and the length of pathologic areas were measured using a light microscope.

Results

Gross anatomy did not demonstrate any abnormality in six tendons. Five tendons were flattened, two had partial tears, none had a complete tear, and two were thickened. Based on MR images flattening of three tendons and both thickened tendons were diagnosed correctly. Reader 1 (R1) diagnosed one of the partial tears, reader 2 (R2) none. In the macroscopically normal tendons (n=6) R1 diagnosed thickening and flattening in one tendon each. R2 diagnosed thickening in three and one tendon, respectively. Three tendons were evaluated as normal on MR images by both readers, one of which was flattened macroscopically. The readers agreed on the presence of any type of diameter alteration in 11 of 15 tendons based on MR images. Interreader agreement concerning the type of diameter alteration was strong (intraclass correlation coefficient [ICC], 0.819, p=0.001). Agreement between gross anatomy and MR imaging was moderate to strong (ICC: R1/R2; 0.722/0.814; p: 0.011/0.002). Histologically, mucoid degeneration (Figure 2) was found in 13 tendons, lipoid degeneration in seven, and fatty infiltration in six. Areas with mucoid degeneration were significantly (Wilcoxon signed rank test) hyperintense with respect to areas with fat infiltration in T2w fs sequences (p=0.025), and significantly hyperintense compared to magic angle artifacts in PDw fs sequences (p=0.034). Areas with fatty infiltration were significantly hyperintense compared to areas with magic angle artifacts in T2w fs (p=0.026) and PDw fs (p=0.046) sequences. There was a good agreement between MR imaging and histology with regard to the location of tendon degeneration. Signal changes without histological correlate (magic angle artifacts) (n=4) were short (max. 7 mm), well demarcated, located exclusively in the curved part of the tendon (segment 3) and not visible on T2w fs images. If a diameter alteration was present, there was always tendon degeneration histologically. None of the specimens demonstrated isolated tendinopathy in segment 1. Segment 1 and 2 demonstrated always the same histologic changes. Interreader agreement concerning the precise end (especially in segment 4) of a caliber change or signal change was considerably inferior to the agreement concerning the precise beginning of a lesion.

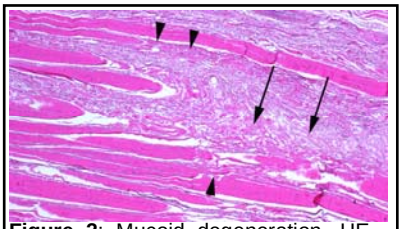

Figure 2: Mucoid degeneration. HE stained mucoid degeneration in light microscopy at 4x magnification. Fragmented and discontinuous tendon fibers (arrows) and newly built intratendinous ground substance (arrowheads).

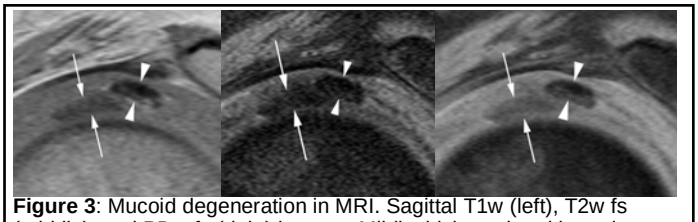

Figure 3: Mucoid degeneration in MRI. Sagittal T1w (left), T2w fs (middle), and PDw fs (right) images. Mildly thickened and hyperintense biceps tendon (arrows) next to the anterior aspect of the supraspinatus tendon (arrowheads). Signal changes were rated grade 2 in T1w, grade1 in T2w fs, and grade 1-2 in PDw fs images.

Conclusion

Caliber changes of the biceps tendon are a specific criterion for tendinopathy but lack sensitivity. Signal changes in the biceps tendon are useful in the diagnosis of tendinopathy although none of the employed sequences in isolation demonstrated histological changes precisely. Interpretation of signal changes needs to account for the different characteristics of the tendon segments. Evaluation of the biceps tendon in segment 1 is often handicapped by anatomical variants. Since none of the specimen had exclusive degenerative changes in segment 1 and degenerative changes in segment 1 were never different to segment 2 we recommend evaluating signal intensity in segment 2 mainly. Concordant assessments on T1w and PDw fs sequences resulted in the most accurate diagnosis of tendinopathy. T2w fs sequences were less sensitive. Segment 3 suffers from magic angle artifacts. If hyperintense tendon areas in segment 3 are not short, sharp defined, and show also signal changes in T2w fs images, degeneration is more probably than an artifact.